

THICKNESS EFFECT ON THE PHYSICAL PROPERTIES OF RF SPUTTERED In_2Te_5 THIN FILMS

Y. F. YUAN^a, L. CHENG^a, Y. P. LI^b, C. M. LIU^a, J. SU^a, L. H. YUAN^a,
X. R. CAO^a, J. LI^{a,c,*}

^a*Department of Optical Science and Engineering, Fudan University, Shanghai 200433, China,*

^b*Shanghai Institute of Technical Physics, Chinese Academy of Sciences, Shanghai 201204, China*

^c*Shanghai Ultra-Precision Optical Manufacturing Engineering Center, Shanghai 200433, China*

The annealed In_2Te_5 films were prepared by the magnetron sputtering method and thermal treatment with thickness from 44 nm to 369 nm. The XRD results reveal that all the films were polycrystalline with preferred orientation in (002) and (-131) plane. The transmittance exhibits high in near-infrared region. The absorption edge of the films shifts toward longer wavelength with the thickness increase. A Spectroscopic Ellipsometer was employed to measure the optical constants of the sample films. In the meantime, the nonlinear optical characterization of the films was studied by the open-aperture Z-scan technique. The change from SA into RSA as the film thickness increases which should be related with the unsaturated defects decreases and the free carrier absorption.

(Received August 21, 2017; Accepted October 23, 2017)

Keywords: Polycrystalline In_2Te_5 film, Thickness effect, Nonlinear optical characteristics

1. Introduction

Recently, the chalcogenide glass has been the focus of intensive research due to their outstanding electrical and optical properties [1]. Owing to relatively wide transparency window [2], low-energy phonons [3], photo-induced phenomena [4] and both high linear and nonlinear refractive indices [5], all of these features make chalcogenide glass of significance in advancing the next generation photonic chip platform for ultrafast all-optical signal processing [6-9]. Indium telluride as binary chalcogenide is a well-known direct band gap semiconductor with defect structure [10, 11]. It has always been regarded as a kind of ideal material for radiation detector, switching and photovoltaics [12, 13]. However, there are no descriptions in a literature about the In_2Te_5 film up to now. Thus it is necessary to investigate the physical properties of In_2Te_5 thin films. On the other hand, it has been found many factors such as composition, thermal treatment and film thickness, can affect the physical properties of chalcogenide. With respect to the thickness dependence effect on the properties of other chalcogenide films, it has been found that the optical parameters are strongly affected by the film thickness changes [14-18]. However, there are few investigation about the effect on the physical properties of In_2Te_5 thin films.

In this work, the In_2Te_5 thin films were fabricated by the magnetron sputtering method and annealed in nitrogen with different thickness ranging from 44 nm to 369 nm. The thickness dependence effect on the In_2Te_5 thin films has been investigated. Furthermore, the micro-structural, physical and optical properties of the films have also been discussed.

*Corresponding author: lijing@fudan.edu.cn

2. Experimental

The In_2Te_5 film samples were deposited on both single-crystalline Si(100) and fused quartz substrates by the magnetron sputtering technique at room temperature. The substrates were cleaned using an ultrasonic cleaner according to the standard cleaning process. The purity of target In_2Te_5 is about 99.999%. The background vacuum of the chamber was approximately 7×10^{-6} mbar, and the working pressure was about 2.8×10^{-3} mbar. The sputtering power of the In_2Te_5 target was controlled at 70 W in radio-frequency mode. For different deposition cycles, the sputtering time was set at 150s, 300s, 450s, 600s, 750s and 900s, respectively. To obtain the crystallinity films, the films were annealed for 1h in flowing nitrogen at 350°C .

The thickness of In_2Te_5 films were determined by SEM measurement. The Raman spectra of the films were tested by Raman micro-spectroscopy (Nanofinder 30). The In_2Te_5 films were detected by X-ray diffractometer (XRD) (Bruker D8 Advance) with Cu-K α ($\lambda = 1.54056 \text{ \AA}$) radiation. The diffraction angles were set from 10° to 60° at 0.02° interval each step. The optical transmission spectra were obtained by using an UV-VIS-NIR (Lambda 1050) spectrophotometer in the wavelength range from 400 nm to 2500 nm. The Spectroscopic Ellipsometer (V-VASE) was employed to measure the films optical parameters. In the measurements of third-order nonlinear optical properties, a Ti: sapphire laser (Spectra Physics, Spitfire Ace) with pulse duration of 100 fs at the repetition rate of 1 kHz was used as the excitation light source with the operating wavelength of 800 nm. In the section of open-aperture (OA) Z-scan process, proper control of the incident laser intensity, which is equivalent to the laser power density I_0 of 60 GW/cm^2 , so that thermal effect and damage to the samples could be avoided.

3. Results and discussion

The Raman spectra of the sample film with sputtering time of 900s was collected to show in Fig. 1. The energy range of vibrations extends to around 300 cm^{-1} . This indicates the similarity in mass and bond forces among the two elements of In and Te. The main Raman peaks around at 111 cm^{-1} , 130 cm^{-1} and 149 cm^{-1} are related to the In-Te phase which is consistent with other works [10, 19]. The inset shows a cross sectional SEM image of the films with the deposition times of 150s and 900s. The corresponding film thickness with different deposition times were shown in Table 1.

Table 1. The thickness, E_g and β_{eff} for the In_2Te_5 films

Sputtering time (s)	Thickness (nm)	E_g (eV)	β_{eff} (cm/GW)
150	44	1.52	-1050
300	100	2.06	336
450	162	1.99	217
600	220	1.95	168
750	285	1.84	112
900	369	1.74	70

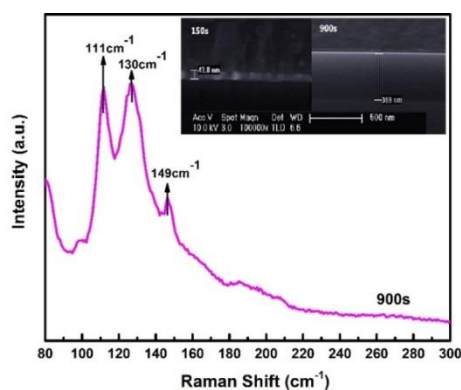


Fig. 1. Raman spectra for the In_2Te_5 film with deposition time of 900s. The inset shows a cross sectional SEM image of the films with deposition times of 150s and 900s.

The structural features of all the films were analyzed according to the XRD pattern and shown in Fig. 2. The results reveal sharp Bragg peaks, indicating the highly polycrystalline. The observed (002), (511), (-131) and (220) peaks were identified as tetragonal In_2Te_5 structure. The preferential orientation of the films in (002) and (-131) planes were obviously observed. It is also observed that the sharpness and intensity of the preferential orientation is enhancement with increasing film thicknesses from 44 nm to 220 nm which reveal an improvement in the crystallinity owing to decrement in disorderliness. Despite the fact, the film thicknesses of 285 nm and 369 nm are found to decrease as compared to that of 220 nm which should be attributed to the stacking of smaller grains on the larger grains. The results are well agreed with the previously research works [16, 17]. The appearance of these crystallites can create defects in the investigated films, it will lead to changes in the optical parameters [14].

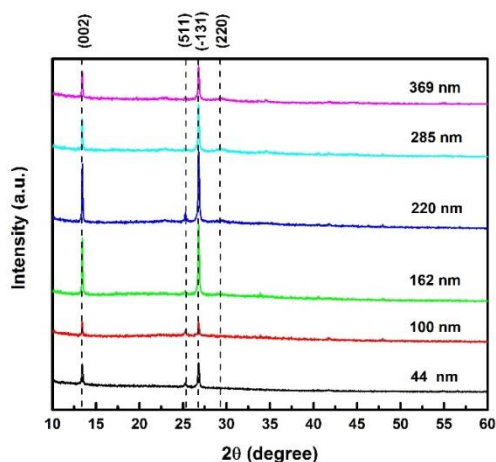


Fig. 2. XRD spectra of the annealed In_2Te_5 films with different thickness

As a function of wavelength, the optical transmission spectra of the In_2Te_5 films with different thicknesses are shown in Fig. 3. The spectrum range is from 300 nm to 2500 nm. Obviously, the transmittance spectra of the films varied significantly with film thickness. It is observed that the transmittance of the films in visible light region is lower than in the near-infrared light region. Furthermore, the absorption edge of the films shifts toward longer wavelengths (red-shift) with the thickness increase. It means a decrease in the optical band gap with increasing film thickness. The interference oscillations become more pronounced with thickness greater than 100 nm which indicates a good homogeneity in the grain shape. Moreover, the transmittance is

between from 50% to 90% in near-infrared region which allows this chalcogenide materials to have various applications in infrared fiber optics and other infrared systems [20]. Moreover, it is clear that the thickness can be as an effective mean for tunable of transmittance.

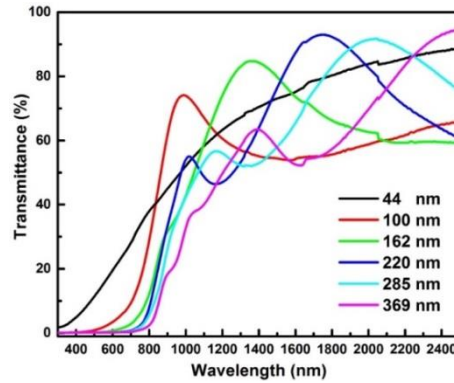


Fig. 3. Transmittance spectra of the annealed In_2Te_5 films with different thickness

Both of refractive index (n) and extinction coefficient (k) curves for the as-deposited and annealed In_2Te_5 films are given in Fig. 4. It is clear that there is an inverse relation between the n and k . The value of n increases firstly, then decreases, finally it remains almost constant with the increase of wavelength. The initial rapid increase of n indicates a rapid change in the absorption energy of the material [15]. At longer wavelength, the value of n decrease indicates normal dispersion of the In_2Te_5 films. The value of k in initially decreases sharply and then it reduces slowly until it reaches around zero at the wavelength of ~ 900 nm. The n has higher values about 3.1-4.2 in the weak absorption region. It should be as a result of the resonance effect between the incident photons and the electron polarization which causes coupling of electrons in the oscillating electromagnetic field [21]. In near-infrared region, the values of k don't change very much with the wavelength. The high n is good indicators for integrated optics. The study of k is extremely important as the prepared material for applications in photo-sensor, photo-electronic, phase transition material, memory devices etc.[22]

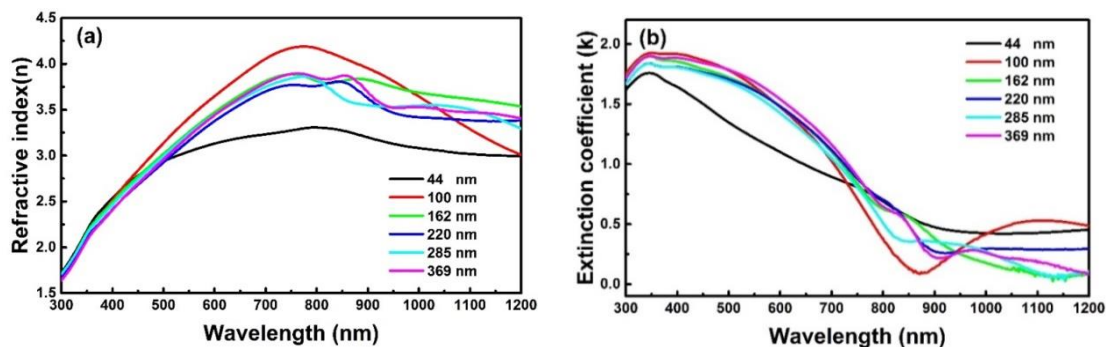


Fig. 4. (a) Refractive index (n) curves of the films.

(b) Extinction coefficient (k) curves of the films

The absorption coefficient α plays as an important parameter in the constants calculation of semiconductor films. It can be calculated from the extinction coefficient k by the following formula [23],

$$\alpha = 4\pi k/\lambda \quad (1)$$

As the thickness increase, the energy level seems to be changed which is due to the incorporation of new energy states or the change of defects. The optical band gap (E_g) of the films can be investigated using Tauc relation [24],

$$\alpha h\nu = A(h\nu - E_g)^n \quad (2)$$

where $h\nu$ is the photon energy, A is a constant, n is equal to $1/2$ for direct band gap. The optical band gap E_g is obtained by extrapolating the linear portion of the plot to the energy axis. The plot of variation of $(\alpha h\nu)^2$ versus $h\nu$ is shown in Fig. 5. The obtained values of the optical band gap are listed in Table 1. It is clear that the decreases from 2.06 eV to 1.74 eV as the thickness increases except the thinnest film. Generally, the dependent of band gap on the thickness can appear due to a large density of dislocation (structural defects) as the thickness increases [18]. These defects can introduce localized states near the band edges leading to an increase in the band tailing width and E_g decreases. The similar behavior has also been observed for other chalcogenide thin films [25-27].

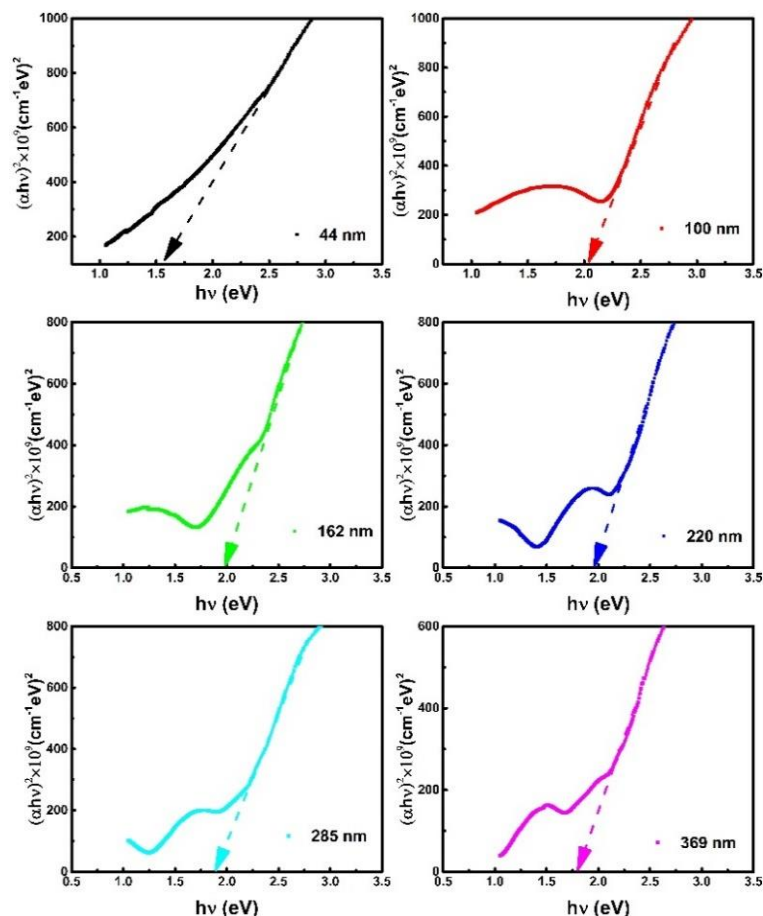


Fig. 5. The optical band gap of the annealed In_2Te_5 films with different thickness

For a better understanding the optical properties of the films with different thicknesses, it is necessary to investigate the dielectric constant. The complex dielectric constant, ϵ

components ($\epsilon_r = n^2 - k^2$) and ($\epsilon_i = 2nk$) are related to the optical constants. The real part (ϵ_r) determines how radiation is refracted while the imaginary part (ϵ_i) relates to absorption of energy due to dipole dislocation [28]. Figure 6 shows the plots of ϵ_r and ϵ_i as a function of photon energy. It is obviously that the ϵ_r have the same behavior as the refractive index n due to the lower value of the extinction coefficient k compared to the n . There was less change in dielectric constant as increasing the thickness except the thinnest film of 44 nm which should be explained on the basis of quantum size effect [17].

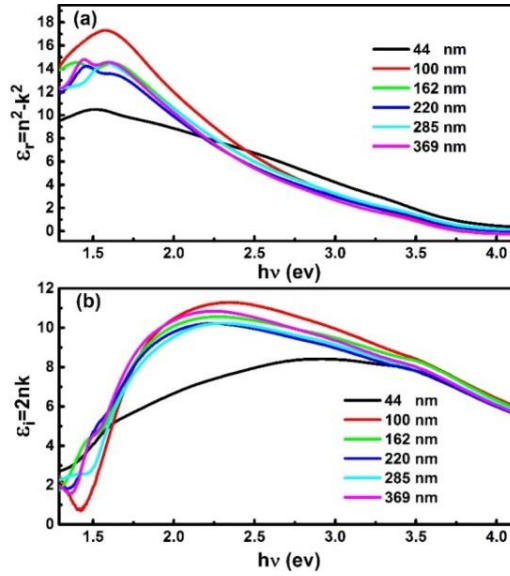


Fig. 6. (a) The real part (ϵ_r) spectra. (b) the imaginary part (ϵ_i) spectra.

The OA Z-scan technique was employed to study the nonlinear optical properties of the In₂Te₅ films with femtosecond laser pulses at the wavelength of 800 nm. No absorption band appears at the measuring wavelength, which implies that the third-order optical nonlinear properties originate from pure electronic distortion with ultrafast response time. In order to ensure that no permanent photo-induced change on the sample has occurred during laser irradiation, we have repeated the experiment by illuminating the sample on the same position. The OA Z-scan results of the films were tested under the incident intensity I_0 of about 60 GW/cm², it is shown in Fig. 7. It is clear that the thinnest film sample exhibits obviously saturation absorption (SA) and other films with different thicknesses indicate reverse saturation absorption (RSA). It observed that the RSA become weaken as the thickness increase. Generally, SA occurs only in semiconductors with band gaps smaller than the incident photon energy, resulting from the electrons excitation from valence band to conduction band, and then Pauli-blocking induced bleaching effect [29]. The change from SA into RSA as the film thickness increases which should be related with the unsaturated defects decreases and the free carrier absorption. The similar behavior appear in other work [11].

The raw data are fitted by using typical OA Z-scan theory proposed by Sheik-Behae. The nonlinear absorption coefficient β_{eff} , defined as $\alpha = \alpha_0 + \beta_{eff}I$, can be calculated by fitting the following equation [8],

$$T_{OA} = \sum_{m=0}^{\infty} \frac{[-\beta_{eff}I_0L_{eff}/(1+z^2/z_0^2)]^m}{(m+1)^{3/2}} \quad (3)$$

where T_{OA} is the normalized transmittance of the OA Z-scan measurement, I_0 is the incident

laser intensity in the focal plane, z is the longitudinal displacement of the samples, z_0 is the Rayleigh length, L_{eff} is the effective thickness of samples which is given by the following expression[7],

$$L_{eff} = \frac{1 - e^{-\alpha_0 L}}{\alpha_0} \quad (4)$$

Here α_0 is the linear absorption coefficient at 800 nm wavelength, and L is the physical thickness of the thin films which is obtained by a step profiler. The obtained values of nonlinear absorption coefficient are shown in Table 1. The absorption coefficient of the RSA films is apparently decrease with the thickness increasing. The absorption coefficient and reverse saturation absorption can be tunable by the thickness in crystalline phases which is important in nonlinear optical application [6-8].

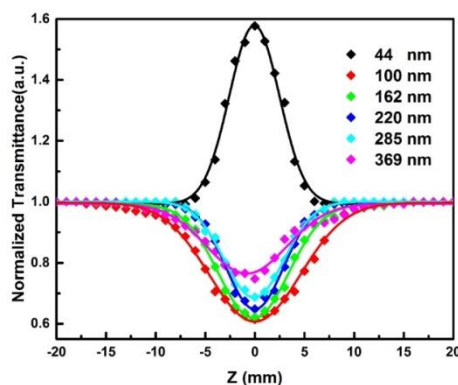


Fig. 7. Open aperture z-scan curves of the annealed In_2Te_5 films with different thicknesses

4. Conclusions

In this paper, the thickness dependence effect on the physical properties of the annealed In_2Te_5 films has been investigated. The film samples were prepared by using the magnetron sputtering method. The corresponding film thicknesses obtained by SEM. The XRD analysis reveals that all the films are polycrystalline in nature exhibit a tetragonal crystalline with preferred orientation in (002) and (-131) planes. The transmittance studies are useful for application in infrared fiber optics and other infrared systems. The Spectroscopic Ellipometry analysis shows that the high refractive index n is good indicators for integrated optics. The optical band gap decreases from 2.21 eV to 1.74 eV as the thickness increases. Nonlinear optical characterization of the films measured by the Z-scan technique, it shows the change from SA into RSA as the film thickness increases which should be related with the unsaturated defects decreases and the free carrier absorption. Our work reveals that the thickness is an effective tool to modulate the structural, physical and optical properties of In_2Te_5 films. Moreover, the In_2Te_5 film demonstrates as a promising semiconductor material for optical limiting application.

Acknowledgements

The authors would like to express their sincere thanks for the financial supports by the funding under Grant Nos. 17ZR1402200, 13ZR1402600, 60578047 and 61427815. The authors thank Prof. L. Y. Chen for effective backup.

Reference

- [1] A. V. Kolobov, P. Fons, A. I. Frenkel, A. L. Ankudinov, J. Tominaga, T. Uruga, *Nature Materials*. **3**(10), 703 (2004).
- [2] B. Bureau, X. H. Zhang, F. Smektala, J.-L. Adam, J. Troles, H.-l. Ma, C. Boussard-Plèdel, J. Lucas, P. Lucas, D. Le Coq, M. R. Riley and J. H. Simmons, *Journal of Non-Crystalline Solids*. **345**, 276 (2004).
- [3] A. Zakery and S. R. Elliott, *Journal of Non-Crystalline Solids*. **330**, 1 (2003).
- [4] Arnaud Zoubir, Martin Richardson, Clara Rivero, Alfons Schulte, Cedric Lopez and K. Richardson, *Optics Letters*. **29**(7), 748 (2004).
- [5] H. T. Guo, C. Q. Hou, F. Gao, A. X. Lin, P. F. Wang, Z. G. Zhou, M. Lu and W. Wei, *Optics Express*. **18**(22), 23275 (2010).
- [6] Q. Liu and X. Zhao, *Journal of Non-Crystalline Solids*. **356**(44), 2375 (2010).
- [7] R. Tintu, V. P. N. Nampoori, P. Radhakrishnan and S. Thomas, *Journal of Applied Physics*. **108**(7), 073525 (2010).
- [8] L. Chen, F. Chen, S. Dai, G. Tao, L. Yan, X. Shen, H. Ma, X. Zhang and Y. Xu, *Materials Research Bulletin*. **70**, 204 (2015).
- [9] G. Lenz, J. Zimmermann, T. Katsufuji, M. E. Lines and H. Y. H. , *Optics Letters*. **25**(4), 254 (2000).
- [10] M. Emziane, J.C. BerneÁdea, J. Ouerfellia, H. Essaidib and A. Barreau, *Materials Chemistry and Physics*. **61**, 229 (1999).
- [11] J. Wang, F. Jin, X. Cao, S. Cheng, C. Liu, Y. Yuan, J. Fang, H. Zhao and J. Li, *RSC Adv*. **6**(105), 103357 (2016).
- [12] K. R. Murali, C. Vinothini and K. Srinivasan, *Materials Science in Semiconductor Processing*. **15**(2), 194 (2012).
- [13] R. Biswas, P. Deb and S. Das, *Optical Materials*. **47**, 586 (2015).
- [14] M. Mohamed and M. A. Abdel-Rahim, *Vacuum*. **120**, 75 (2015).
- [15] Y. Ji, Y. Ou, Z. Yu, Y. Yan, D. Wang, C. Yan, L. Liu, Y. Zhang and Y. Zhao, *Surface and Coatings Technology*. **276**, 587 (2015).
- [16] A. Purohit, S. Chander, S. P. Nehra, C. Lal and M. S. Dhaka, *Optical Materials*. **47**, 345 (2015).
- [17] N. Khedmi, M. B. Rabeh, D. Abdelkadher, F. Ousgi and M. Kanzari, *Crystal Research and Technology*. **50**(1), 69 (2015).
- [18] M. I. Abd-Elrahman, R. M. Khafagy, S. A. Zaki and M. M. Hafiz, *Materials Science in Semiconductor Processing*. **18**, 1 (2014).
- [19] F. L. Faight, K. Ersching, J. J. S. Acuña, C. E. M. Campos and P. S. Pizani, *Materials Chemistry and Physics*. **130**(3), 1361 (2011).
- [20] H. Nyakoty, T. S. Sathiaraj and E. Muchuweni, *Optics & Laser Technology*. **92**, 182 (2017).
- [21] A. S. Hassanien and A. A. Akl, *Journal of Alloys and Compounds*. **648**, 280 (2015).
- [22] A. A. Mulama, J. M. Mwabora, A. O. Oduor, C. M. Muiva, B. Muthoka, B. N. Amukayia and D. A. Mbeti, *New Journal of Glass and Ceramics*. **5**(2), 16 (2015).
- [23] J C Manifacier, J Gasiot and J. P. Fillard, *Journal of Physics E*. **9**(11), 1002 (1976).
- [24] J. Tauc and A. Menth, *Journal of Non-Crystalline Solids*. **8**(10), 569 (1972).
- [25] P. Sharma and S. C. Katyal, *Materials Letters*. **61**(23), 4516 (2007).
- [26] M. I. Abd-Elrahman, A. Y. Abdel-Latif, R. M. Khafagy, N. Younis and M. M. Hafiz, *Materials Science in Semiconductor Processing*. **24**, 21 (2014).
- [27] M. I. Abd-Elrahman and M. M. Hafiz, *Journal of Alloys and Compounds*. **551**, 562 (2013).
- [28] P. Sharma and S. C. Katyal, *Applied Physics B*. **95**(2), 367 (2009).
- [29] M. Rumi and J. W. Perry, *Advances in Optics and Photonics*. **2**(4), 451 (2010).